Intermolecular Potential Energy Surface for CS2 Dimer

ARTICLE *in* JOURNAL OF COMPUTATIONAL CHEMISTRY · APRIL 2011

Impact Factor: 3.59 · DOI: 10.1002/jcc.21658 · Source: PubMed

4 AUTHORS, INCLUDING:

Mansoor Namazian
Yazd University
58 PUBLICATIONS **1,249** CITATIONS
SEE PROFILE

Michelle L Coote
Australian National University
214 PUBLICATIONS **5,674** CITATIONS
SEE PROFILE

Intermolecular Potential Energy Surface for CS_2 Dimer

HOSSEIN FARROKHPOUR,[1] ZAINAB MOMBEINI,[1] MANSOOR NAMAZIAN,[2] MICHELLE L. COOTE[2]
[1]*Department of Chemistry, Isfahan University of Technology, Isfahan 84156-83111, Iran*
[2]*ARC Centre of Excellence for Free-Radical Chemistry and Biotechnology, Research School of Chemistry, Australian National University, Canberra ACT 0200, Australia*

Received 23 January 2010; Revised 10 July 2010; Accepted 6 August 2010
DOI 10.1002/jcc.21658
Published online 12 October 2010 in Wiley Online Library (wileyonlinelibrary.com).

Abstract: A new four-dimensional intermolecular potential energy surface for CS_2 dimer is obtained by *ab initio* calculation of the interaction energies for a range of configurations and center-of-mass separation distances for the first time. The calculations were performed using the supermolecular approach at the Møller–Plesset second-order perturbation (MP2) level of theory with the augmented correlation consistent basis sets (aug-cc-pV*x*Z, x = D, T) and corrected for the basis-set superposition error using the full counterpoise correction method. A two-point extrapolation method was used to extrapolate the calculated energy points to the complete basis set limit. The effect of using the higher levels of theory, quadratic configuration interaction containing single, double, and perturbative triple excitations QCISD(T) and coupled cluster singles, doubles and perturbative triples excitations CCSD(T), on the shape of potential energy surface was investigated. It is shown that the MP2 level of theory apparently performs extremely poorly for describing the intermolecular potential energy surface, overestimating the total energy by a factor of nearly 1.73 in comparison with the QCISD(T) and CCSD(T) values. The value of isotropic dipole–dipole dispersion coefficient (C_6) of CS_2 fluid was obtained from the extrapolated MP2 potential energy surface. The MP2 extrapolated energy points were fitted to well-known analytical potential functions using two different methods to represent the potential energy surface analytically. The most stable configuration of the dimer was determined at R = 6.23 au, $\alpha = 90^\circ$, $\beta = 90^\circ$, and $\gamma = 90^\circ$, with a well depth of 3.980 kcal mol^{-1} at the MP2 level of theory. Finally, the calculated second virial coefficients were compared with experimental values to test the quality of the presented potential energy surface.

 J Comput Chem 32: 797–809, 2011

Key words: CS_2 dimer; Møller–Plesset second-order perturbation (MP2); QCISD(T); CCSD(T); potential energy surface; extrapolation; basis-set superposition error; isotropic dipole–dipole dispersion coefficient

Introduction

Intermolecular interactions play a central role in governing the thermodynamic and transport properties of gases, liquids, and solids. Molecular dynamic simulation is an important tool for predicting structural information as well as thermodynamic and transport properties of condensed matter. However, the accuracy of the results obtained from molecular dynamic simulation depends on the reliability and precision of the used intermolecular interaction potential.

Generally, there are two methods available for obtaining intermolecular interaction potential. The first involves the use of experimental equilibrium and nonequilibrium thermodynamic data such as the second virial coefficient, compressibility factor, and viscosity to parameterize a mathematical function describing the potential. However, two major difficulties are associated with this method: (1) each thermodynamic property is related to a certain region of the potential energy surface and (2) the anisotropy of the potential energy surface cannot be determined. The second method involves the use of *ab initio* molecular orbital theory calculations, in conjunction with various approximations, to calculate the energy directly as a function of geometry. Although this approach provides coverage of the entire potential energy surface, its accuracy and reliability is limited by the theoretical level of calculation used, the basis set incompleteness, and the quality of the approximations made.

CS_2 is an important solvent used in supercritical fluid extraction[1]; hence, there is a great interest in obtaining accurate intermolecular interaction potential for modeling its structure and properties and in predicting its phase transitions. CS_2 is highly flammable, having one of the lowest autoignition temperatures

Correspondence to: H. Farrokhpour; e-mail: farrokhphossein@gmail.com

Contract/grant sponsor: Isfahan University of Technology Research Council

Contract/grant sponsor: Australian Research Council

(90°C) of all solvents. As a result of this reactivity and instability, apertures fail during the collection of *P-V-T* data in high-temperature experiments, making it difficult to measure its thermodynamic properties at high temperatures. The second virial coefficients of CS_2 have been measured previously over a limited range of temperature (280–470 K), but are subject to a large uncertainty.[2] For example, the latest set of measurements by Hajjar et al.[3] are up to 100 $cm^3\ mol^{-1}$ less negative than previous results, particularly at high temperatures.[2] Given these experimental difficulties, in this work we use the *ab initio* molecular orbital theory to calculate the potential energy surface of CS_2 dimer and use it to calculate the second virial coefficient.

Zhu et al.[4] proposed a three-centre site–site Lennard-Jones (LJ) plus Coulomb potential for CS_2 dimer. The parameters of the potential function are obtained using experimental values of configurational energy, and the cross-interaction parameters, in the site–site potential, are calculated using the usual combining rules in thermodynamics. Hoinkis et al.[5] studied the intermolecular potential for CS_2, N_2, Ar, Ne, He, CO_2, CO, and HCl using an approximation of the self-consistent field (SCF) method in which the SCF potential is represented by a site–site potential V of (exp, $1/R$)-type, which accounts for the exchange plus penetration and the long-range Coulomb forces by means of a point charge model. Using this method, Peebles and Peebles[6] calculated the intermolecular potential between CS_2 and dimethyl ether dimer to obtain the best configuration of the dimer. They found that CS_2 is aligned roughly perpendicular to the dimethyl ether dimer heavy atom plane. Although there have been several previous theoretical studies on the potential energy surface of CO_2 dimer in the literature,[7–12] to the best of our knowledge, there has as yet been no *ab initio* calculation of the intermolecular interaction of CS_2 dimer using post-SCF methods.

In this work, we use high-level *ab initio* molecular orbital theory calculations to calculate the intermolecular potential energy surface of CS_2 dimer, its second virial coefficient, and isotropic dipole–dipole dispersion coefficient (C_6). To this end, we have used Møller–Plesset second-order perturbation (MP2)[13] theory in conjunction with the aug-cc-pVxZ, x = D, T basis sets developed by Dunning et al.[14] and basis-set superposition error (BSSE) using the full counterpoise (CP) correction method, for computing energy values expected at the limit of complete basis via a two-point extrapolation procedure. The extrapolated MP2 potential energy surface is fitted using a four-dimensional (4D) analytical expression to describe the topology of the potential energy surface and calculate the second virial coefficient of CS_2 fluid. Also, the value of the isotropic dipole–dipole dispersion coefficient (C_6) of CS_2 fluid is calculated from the extrapolated MP2 potential energy surface and compared with that obtained from other theoretical method in the literature. The extrapolated MP2 intermolecular potential of four dimer configurations (cross, parallel, T-shape, and linear), obtained at different intermolecular distance, will be compared with those obtained from the calculations at the higher quadratic configuration interaction containing single, double, and perturbative triple excitations (QCISD(T)) and coupled cluster singles, doubles and perturbative triples excitations CCSD(T) levels of theory. Finally, the extrapolated potential energy surface at the QCISD(T) level of theory will be approximated by scaling the extrapolated MP2 potential energy surface.

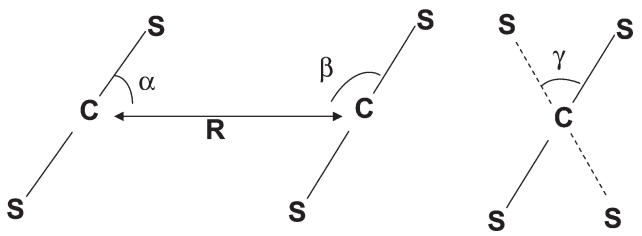

Figure 1. Definition of the dimer structure.

Methodology

Geometry optimization of a single carbon disulfide molecule was performed at the MP2 level of theory using the Gaussian 03 program suite.[15] A variety of basis sets, including 6-311+G, 6-311+G*, cc-pVDZ, cc-pVTZ, aug-cc-pVDZ, and aug-cc-pVTZ, were used for geometry optimization. The optimized C-S bond length for aug-cc-pVTZ basis set was found to be 2.9534 au, which is close to its reported experimental value (2.9349 au).[16] Therefore, the C-S bond length in the monomer was kept at the experimental value for all calculations in this work.

Under a rigid-rotor approximation, the intermolecular potential energy of CS_2 dimer is a function of four variables: the distance R between two carbon atoms (the center of mass of two monomers), the angles α and β between the vector $\boldsymbol{R}$, and the axis of the respective molecules A and B, and a dihedral angle γ (Fig. 1). The angles α, β, and γ vary between 0° and 180°. These angles are sufficient to determine completely all possible relative orientations of two CS_2 monomers. The distance R varies between 2.5 and 15 Å in steps of 1 Å for 8–15 Å and 0.1 Å for 2.5–8 Å. Different angular orientations have been selected by changing the angles α, β, and γ in steps of 30°.

CS_2 molecule has a center of symmetry, and its potential energy surface, denoted by E (α, β, γ, R), has the following symmetry properties:

$$E(\alpha,\beta,\gamma,R) = E(\pi-\alpha,\beta,\pi-\gamma,R) \quad (1)$$

$$E(\alpha,\beta,\gamma,R) = E(\alpha,\pi-\beta,\pi-\gamma,R) \quad (2)$$

In addition, both molecules are interchangeable:

$$E(\alpha,\beta,\gamma,R) = E(\beta,\alpha,\gamma,R) \quad (3)$$

These symmetry properties lead to a reduction in the range of the angles that have to be covered by *ab initio* calculations. In this case, the angles α and β vary between 0° and 90°. By considering the above symmetry properties, 2790 independent points of the intermolecular energy surface have been calculated within the supermolecular approach at the MP2 level of theory using augmented correlation consistent basis sets (aug-cc-pVxZ, x = D, T). MP2 level of theory was chosen because it is well known to offer an excellent compromise between accuracy and computational cost, and usually (though not

always[17,18]) provides an excellent approximation compared with the considerably more expensive methods such as MP4 or CCSD(T).

BSSE has an important role in evaluating the interaction energy using the supermolecular approach. The BSSE arises from an improved description of each monomer in the presence of the basis of the other fragment. An obvious strategy for solving this problem, suggested by Boys and Bernardi,[19] is to carry out all calculations—those on the fragments as well as those on the complex—on the same combined atomic basis. The intermolecular potential energy calculated in this manner is known as the CP-corrected intermolecular potential energy and obtained as follows:

$$\Delta E_{AB}^{CP} = E_{AB} - E_A^{CP} - E_B^{CP} \quad (4)$$

Here, ΔE_{AB}^{CP} is the corrected intermolecular potential energy, ΔE_A^{CP} and ΔE_B^{CP} are the CP energies of monomers *A* and *B*, respectively, calculated fully on the basis of the supermolecular *AB*. According to Eq. (4), three *ab initio* calculations are required for each point of the potential surface (except when $\alpha = \beta$ where the monomer energies ΔE_A^{CP} and ΔE_B^{CP} are identical, which allows one computation to be omitted).

The basis set incompleteness is one source of error that limits the ultimate accuracy of the results, specially when electron correlation methods such as MP2 and QCISD(T) are used for *ab initio* calculations.[20] In this case, the basis set convergence is slow, whereas the convergence of the Hartree Fock (HF) energy is considerably quicker than the correlation energy. The reason for the slow convergence of the correlation energy is the difficulty in describing the short-range electronic interactions.[21] In this work, the correlation part of the MP2 and QCISD(T) interaction energies, obtained using the aug-cc-pVDZ and aug-cc-pVTZ basis sets, were extrapolated to the complete basis set (CBS) limit, and the HF energy part was not extrapolated but taken from the aug-cc-pVTZ calculations. The details of the extrapolation method and its effect on the calculated intermolecular potential energy will be discussed in extrapolation scheme subsection.

Results and Discussion

Effect of Basis Set

The intermolecular potential energies of CS_2 dimer for the parallel configuration ($\alpha = \beta = 90^\circ$ and $\gamma = 0^\circ$), which are calculated using several basis sets at the MP2 level of theory, are shown in Figure 2 for an illustration of the basis set effect. The basis sets used for calculation are cc-pV*x*Z (*x* = D,T) and aug-cc-pV*x*Z (*x* = D, T, Q). It is found that the basic characteristic of the intermolecular potential curve is very sensitive to the type of basis set used in the calculation. Addition of the diffuse functions in the basis set has a great effect so that a larger basis set leads to a more attractive interaction and shifts the minimum position of the potential to shorter intermolecular distances. Also, the collision diameter and repulsive part of the potential shift to shorter intermolecular distances by increasing the size of basis set. Another important point worth noting is the effect of the basis set on the convergence of the potential energy surface.

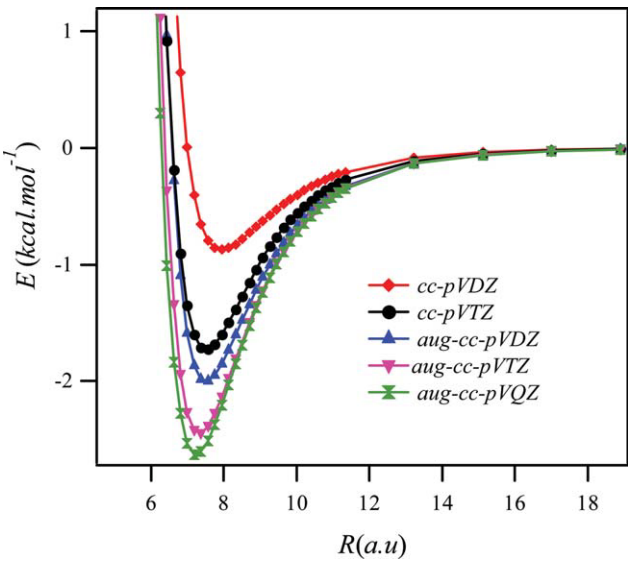

Figure 2. Radial dependence of the intermolecular potential energy, calculated using different basis sets at the MP2 level of theory for the parallel configuration ($\alpha = \beta = 90^\circ$ and $\gamma = 0^\circ$). Counterpoise (CP) correction has been used to eliminate the basis-set superposition error (BSSE). [Color figure can be viewed in the online issue, which is available at wileyonlinelibrary.com.]

It is obvious that the potential energies calculated with aug-cc-pV*x*Z basis sets have a faster convergence than those calculated with cc-pV*x*Z basis sets with increments of the cardinal number of the basis set. Hence, the aug-cc-pV*x*Z basis sets were selected for *ab initio* calculations in this work.

Effect of Geometry Optimization

To investigate the effect of the geometry relaxation of the dimer on the potential energy surface, the intermolecular potential was calculated using optimized values of C-S bond length of dimer. In this case, the C-S bond lengths of two CS_2 monomers were optimized for each value of intermolecular distance during the calculation. The keyword OPT = TIGHT was used to increase the convergence criteria of the software to obtain the reliable optimized dimer geometry. Figure 3a compares the calculated intermolecular potential energy curves using rigid rotor approximation with those obtained using the optimized values of C-S bond length at MP2/aug-cc-pVDZ and TZ level of theory for parallel ($\alpha = 90^\circ$, $\beta = 90^\circ$, and $\gamma = 0^\circ$) and T-shape ($\alpha = 90^\circ$, $\beta = 0^\circ$, and $\gamma = 0^\circ$) configurations, respectively. The maximum difference between the intermolecular potential energy values obtained using rigid rotor approximation and those obtained using the optimized values of C-S bond lengths is 0.003 and 0.004 kcal mol^{-1} for parallel and T-shape, respectively. It is obvious that the effect of C-S bond length variation on the intermolecular potential is negligible. Figure 3b shows the variation of the optimized values of C-S bond length of the dimer structure as a function of *R*, for the configurations in Figure 3a. As shown, the variation not only depends on the dimer configuration but also on the basis set type. It is seen that the optimized

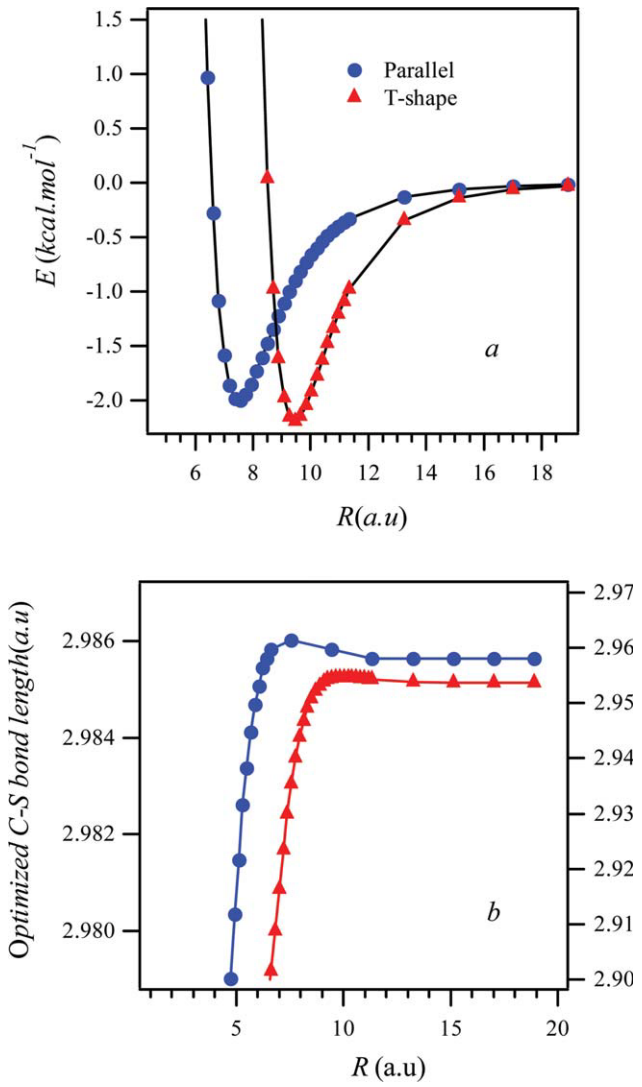

Figure 3. (a) Comparison of the intermolecular potential energy curves, calculated using the fixed C-S bond length (solid lines) at the MP2 level of theory using aug-cc-pVDZ and TZ basis sets for parallel ($\alpha = \beta = 90^\circ$ and $\gamma = 0^\circ$) and T-shape ($\alpha = 90^\circ$ and $\beta = \gamma = 0^\circ$) configurations, respectively with those obtained using the optimized values of C-S bond length (symbols). Counterpoise (CP) correction has been used to eliminate the basis-set superposition error (BSSE). (b) Radial dependence of the optimized values of C-S bond length of dimer, calculated at the MP2 level of theory using aug-cc-pVDZ and TZ basis sets, for parallel (left axis) and T-shape (right axis) configurations, respectively. [Color figure can be viewed in the online issue, which is available at wileyonlinelibrary.com.]

value of C-S bond length decreases at short distances and reaches the corresponding optimized value of the free CS_2 monomer at larger distances. The optimized values of C-S bond length in Figure 3b are close to its experimental value (2.9349 au). Therefore, it is reasonable to fix the C-S bond length at its experimental value. The C-S bond length was kept at its experimental value for all calculations in this work.

Extrapolation Scheme

Generally, there are two different methods for reaching to the CBS limit in the calculation of intermolecular interaction energies. The first method is adding enough number bond basis functions to Gaussian basis sets. This method is very effective in the calculation of interaction energy of weakly bond systems, and the calculated interaction energy converges easily to the complete basis limit by increasing the number of added bond functions.[22] The second method, used in this work, is using an extrapolation method. The use of an extrapolation method for the electron correlation energies, similar to using bond functions, significantly improves the calculated results. It has been shown that using the extrapolation method can recover more than 95% of the exact basis set limit correlation energies, which is obtained by adding bond functions to Gaussian basis sets.[23,24] In this work, we have selected extrapolation method to extrapolate correlation energies to CBS limit.

A simple two-point extrapolation scheme was used for the correlation part of the intermolecular interaction potential[20]:

$$E_{\mathrm{corr}}(L_{\max}) = E_{\mathrm{corr}}(\infty) + BL_{\max}^{-3} \tag{5}$$

where, $E_{\mathrm{corr}}(L_{\max})$ is the correlation energy of a basis set with a small cardinal number $L_{\max}$, and $E(\infty)$ is the extrapolated correlation energy. This extrapolation scheme has been used widely in connection with the cc-pVxZ and aug-cc-pVxZ basis sets. Equation (5) requires the correlation parts of the intermolecular potential calculated with the two different basis sets.

Three different pairs of basis sets, *viz*. (aug-cc-pVDZ and aug-cc-pVTZ), (aug-cc-pVDZ and aug-cc-pVQZ), and (aug-cc-pVTZ and aug-cc-pVQZ), were used separately to obtain the extrapolated values of correlation energies at the MP2 level of theory for parallel configuration. Figure 4a shows the extrapolated correlation intermolecular energies obtained using these three different pairs of basis sets along with Eq. (5). It can be seen that the intermolecular correlation energy increases when the distance between two CS_2 monomer decreases and decreases at large intermolecular separation. This behavior has been observed for all dimer configurations considered in this work. Also, the extrapolated values of correlation energies obtained using these three different pairs of basis sets are very close to each other. This means that the extrapolated correlation energies converge fast, which is confirmed by the inset of the figure. For example, the difference between the extrapolated values of the correlation energy using (aug-cc-pVTZ and aug-cc-pVQZ) and (aug-cc-pVDZ and aug-cc-pVTZ) pairs of basis sets at 7.2 au is about 0.02 kcal mol^{-1}. Also, the inset of the figure shows that we can obtain reasonable extrapolated correlation energies by using aug-cc-pVDZ and aug-cc-pVTZ and, thereby, avoid the use of larger basis sets such as aug-cc-pVQZ.

To illustrate the effect of extrapolation on the correlation intermolecular energy, the calculated correlation part of the potential for the parallel configuration ($\alpha = \beta = 90^\circ$ and $\gamma = 0^\circ$) using aug-cc-pVDZ, TZ, and QZ basis sets, separately, are shown in Figure 4b. It is seen that the aug-cc-pVDZ basis set leads to a lower correlation energy, especially at lower intermo-

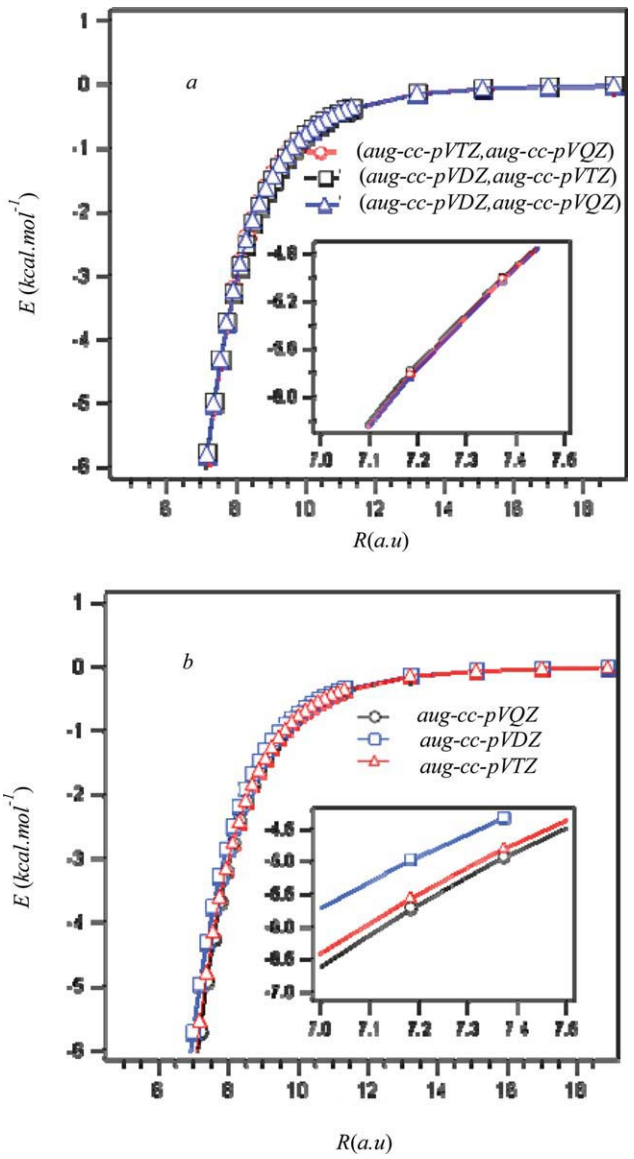

Figure 4. (a) Extrapolated correlation part of the intermolecular potential, calculated at the MP2 level of theory using three pairs of basis sets, for the parallel configuration ($\alpha = \beta = 90^\circ$ and $\gamma = 0^\circ$). (b) Unextrapolated correlation part of intermolecular potential, calculated at the MP2 level of theory, using different basis sets. [Color figure can be viewed in the online issue, which is available at wileyonlinelibrary.com.]

lecular distances, in comparison with those obtained using aug-cc-pVTZ and -QZ basis sets. For example, the difference between the calculated correlation energy using aug-cc-pVDZ and that obtained using aug-cc-pVQZ basis set is about 3.56×10^{-3} kcal mol^{-1} at $R = 13.233$ au, which increases to 0.60615 kcal mol^{-1} at $R = 7.3724$ au. This behavior can be seen in the inset of Figure 4b. Comparison of the inset of Figures 4a and 4b show that the extrapolated correlation energies converge faster than the nonextrapolated energies. As mentioned before, the correlation part of the interaction energies obtained with the aug-cc-pVDZ and aug-cc-pVTZ basis sets were extrapolated to the CBS limit, and the HF energy part was not extrapolated but taken from the aug-cc-pVTZ calculations to obtain the extrapolated interaction energy.

Effect of Theoretical Level on the Shape of Potential Energy Surface

In this part, we investigate the effect of a more computationally intensive quantum chemical method such as QCISD(T) on the potential energy surface. Obviously, using the combination of the QCISD(T) method and such large basis sets as aug-cc-pVxZ (x = D,T) is computationally expensive, especially when 2790 independent points on the potential energy surface are considered for calculation. Instead, the QCISD(T) calculations were performed on the cross ($\alpha = 90^\circ$, $\beta = 90^\circ$, and $\gamma = 90^\circ$) and parallel ($\alpha = 90^\circ$, $\beta = 90^\circ$, and $\gamma = 0^\circ$) configurations. Figure 5 shows the radial dependence of the extrapolated intermolecular potential, calculated at the MP2 and QCISD(T) levels of theory, for parallel and cross configurations. As shown, the MP2 values of energies are overestimated compared with the QCISD(T) values because of the exaggeration of correlation energy, which exists at some levels of MP theory.[25] This behavior is expected to occur in situations with a high degree of electron clustering.[26] As shown in Figure 5, there is almost no change in the position of the minimum by changing the theoretical level of theory from MP2 to QCISD(T) level. For example, the difference between the minimum position of the extrapolated potential, calculated at the MP2 level and corresponding one at the QCISD(T) level, is about 0.35 au for both parallel and cross configurations. Also, the shape of the extrapolated potentials, especially at the well-depth region, which is important in the calculation of thermodynamic properties, as calculated using the two different methods, is almost the same for each of the cross and parallel configurations, separately, although there is a little difference between the position of minimum energy at MP2 and QCISD(T) levels. Therefore, it seems that the shapes of the two extrapolated potential energy surfaces, as calculated at the MP2 and QCISD(T) levels of theory, are similar, and their variations with α, β, γ, and R are almost the same. This means that shape is nearly independent of the theoretical level of theory used. To investigate this further, the normalized minimum values of the extrapolated potentials of parallel, linear, and T-shape configurations relative to the minimum extrapolated interaction energy of cross configuration, calculated at the MP2 level of theory, were compared with those obtained from the QCISD(T) method. The relative interaction energies of parallel, linear, and T-shape, at the minimum position, were found to be 0.65, 0.28, and 0.57, respectively, which are almost equal to the corresponding values obtained from the QCISD(T) method (i.e., 0.66, 0.27, and 0.58). This shows that the shape of the extrapolated potential energy surface at the QCISD(T) level of theory is almost well approximated at the MP2 level of theory.

Although the shapes of potential energy surfaces are approximately similar at the two levels of theory, the contribution of the correlation energy in the calculated MP2 values of energy are more than the corresponding values calculated at the

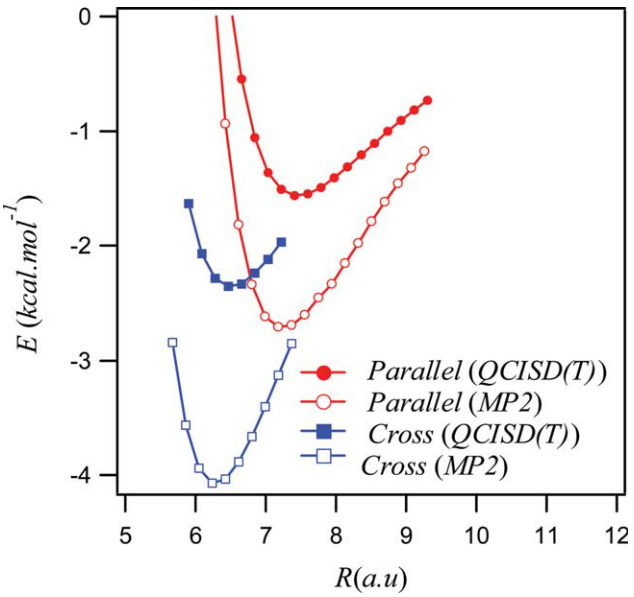

Figure 5. Radial dependence of the extrapolated intermolecular potential to the complete basis, calculated at the MP2 and QCISD(T) levels of theory, for parallel ($\alpha = \beta = 90^\circ$ and $\gamma = 0^\circ$) and cross ($\alpha = \beta = 90^\circ$ and $\gamma = 90^\circ$) configurations.

QCISD(T) level of theory. Because the shapes of potential energy surfaces are approximately the same at MP2 and QCISD(T) levels of theory, the simplest method to resolve this problem is to introduce a scaling factor, η, in the spirit of Domaski et al.[27] and write the intermolecular potential at the QCISD(T) level as follows:

$$E_{\mathrm{QCISDT}}(\alpha, \beta, \gamma, R) = \eta E_{\mathrm{MP2}}(\alpha, \beta, \gamma, R) \qquad (6)$$

Equation (6) means that increasing the quality of the computational level does result in a simple scaling of the potential energy surface in the CS_2-CS_2 system. Because the shape of the potential energy surface at the QCISD(T) level of theory is almost well described at the MP2 level, we can conclude that the scaling factor is independent of the four variables (α, β, γ, and R). The scaling factor for converting the extrapolated MP2 potential energy to QCISD(T) ones for cross, parallel, T-shape, and linear configurations are 0.578, 0.579, 0.570, and 0.587, respectively, which was obtained by dividing the QCISD(T) extrapolated potential at the R minimum to the corresponding value at the MP2 level. It is clear that the scaling factor is almost independent of the dimer configuration. The average value of these four numbers (0.578) has been selected as global scaling factor to approximately estimate the extrapolated QCISD(T) potential energy surface. Figure 6 shows the radial dependence of the extrapolated potential at QCISD(T) level for the parallel and cross configurations compared with the scaled MP2 result, for which the same scaling factor (0.578) has been considered for each value of R. A similar behavior was observed for T-shape and linear configurations. Hence, we may conclude that the scaled MP2 surface offers an excellent approximation to its considerably more expensive QCISD(T) counterpart.

Figure 7 shows the comparison of the radial dependence of the intermolecular potential energies of cross and parallel configurations, calculated at the CCSD(T) level of theory using aug-cc-pVTZ basis set, with those obtained at the QCISD(T) level of theory. As shown, the CCSD(T) values of intermolecular potential are as accurate as those obtained using QCISD(T) method with the same basis set. Therefore, it can be concluded that the scaling factor (0.578) is also valid for converting the MP2 results to CCSD(T) for all of the configurations.

Four-Dimensional Analytical Representation and Topology of Potential Energy Surface

The extrapolated intermolecular potentials, calculated at the MP2 level of theory for different configurations and intermolecular distances, were used to obtain the adjustable parameters of a proposed potential function. An exponential-6 (exp-6) potential was fitted to the extrapolated energies. The functional form of the model potential is expressed as below:

$$E_{\exp-6}(R) = \frac{\varepsilon}{\delta - 6}\left[6\exp\left(\delta\left(1 - \frac{R}{R_{\mathrm{m}}}\right)\right) - \delta\left(\frac{R_{\mathrm{m}}}{R}\right)^6\right] \qquad (7)$$

where R is the distance between the center of mass of molecules, ε is the depth of the attractive well, δ is an adjustable parameter that controls the slope of the repulsive part of the potential, and R_{m} is the value of R at the potential minimum. Exp-6 potential is computationally convenient, and its form is not complicated; thus, it is widely used in molecular dynamic simulation. There are no R^{-8} and R^{-10} terms in this potential model,

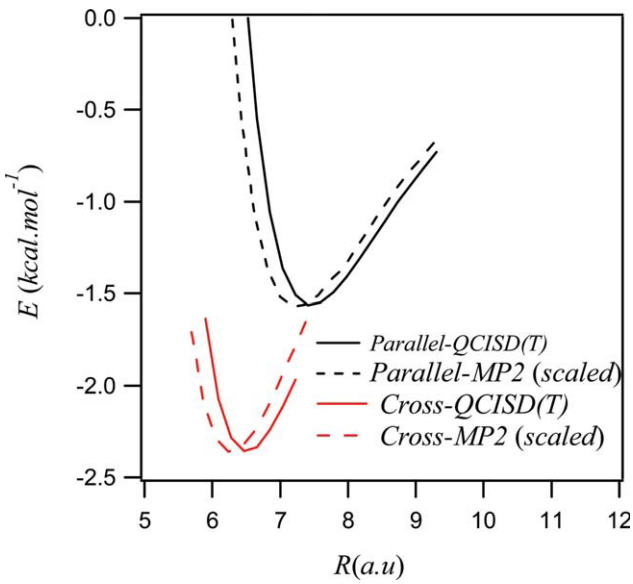

Figure 6. Comparison of the extrapolated intermolecular potential, calculated at the QCISD(T) level of theory with the scaled extrapolated intermolecular potential calculated at the MP2 level of theory for parallel ($\alpha = \beta = 90^\circ$ and $\gamma = 0^\circ$) and cross ($\alpha = \beta = 90^\circ$ and $\gamma = 90^\circ$) configurations.

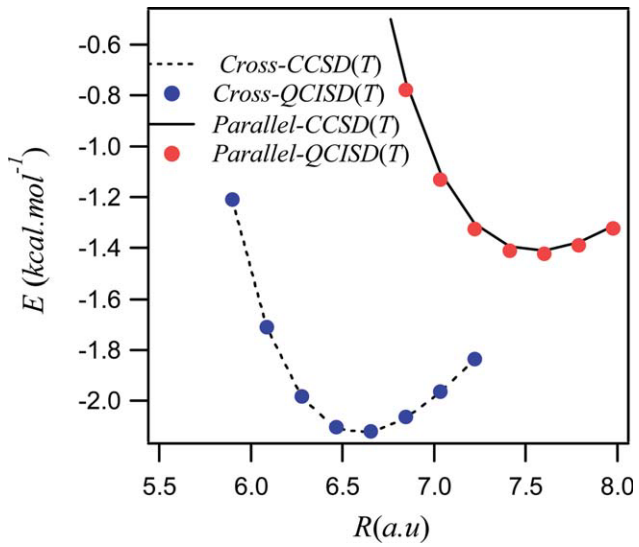

Figure 7. Comparison of the intermolecular potential, calculated at the CCSD(T) level of theory using aug-cc-pVTZ, with the corresponding values obtained using QCISD(T) method with the same basis set for parallel and cross configurations.

but, when it is used for the radial fitting, the R^{-6} term has to be larger to compensate the contribution of R^{-8} and R^{-10} terms at long range. Therefore, the C_6 coefficient of each dimer configuration, which is obtained from the radial fitting, is larger than the true C_6 coefficient (dipole–dipole dispersion coefficient).[28]

The parameters (ε, δ, and R_m) are a series of angular functions $Y_{l_a l_b l}$ (α, β, γ) that show the angular dependency. The general form of the parameters ε, δ, and R_m are as follows:

$$Q(\alpha,\beta,\gamma) = \sum_{l_a}\sum_{l_b}\sum_{|l_a-l_b|}^{l_a+l_b} Q_{l_a l_b l} Y_{l_a l_b l}(\alpha,\beta,\gamma) \qquad (8)$$

$$|l_a - l_b| \le l \le l_a + l_b$$

where, l_a,l_b = 0,2,4,... and Q is ε, δ, and R_m. The angular functions $Y_{l_a l_b l}$ (α, β, γ) are bipolar spherical harmonics[29]

$$Y_{l_a l_b l}(\alpha,\beta,\gamma) = (2l+1)^{1/2}\sum_m (-1)^{l_a - l_b} \times \begin{pmatrix} l_a & l_b & l \\ m & -m & 0 \end{pmatrix} y^m_{l_a}(\alpha,\phi_a) y^{-m}_{l_b}(\beta,\phi_b) \qquad (9)$$

$$\phi_a = 0, \phi_b = \gamma$$

where $y^m_{l_a}$ and $y^{-m}_{l_b}$ are spherical harmonics, the matrix in Eq. (8) is a Wigner 3-j coefficient, and $-\min(l_a,l_b) \le m \le \min(l_a,l_b)$. The fixed values of the parameter $Q_{l_a l_b l}$ are determined through the angular fitting of the potential parameters (ε, δ, and R_m), obtained from the radial fitting of the extrapolated intermolecular potential of all dimer configurations.

Generally, there are two different fitting procedures to obtain the parameters. According to the first method, the angular dependence of potential energy surface at several fixed separations is determined, and, then, the fitting is completed by obtaining the radial dependence. According to the second method, the radial dependence is obtained for several orientations and the obtained parameters are then taken as new functions and expanded according to Eq. (8). In this work, we adopted the second procedure for the fitting of potential energy surface. The initial values of ε and R_m of each configuration is estimated from the plot of the extrapolated potential energy *versus* intermolecular distance. At this stage, the fitting yields values of ε, δ, and R_m for each configuration, and the radial fitting of the potential is completed. The average values of standard deviation in ε, δ, and R_m for all the configurations considered in the radial fitting are about 0.018 kcal mol^{-1}, 0.058, and 0.0148 au, respectively. Linear configuration has the largest standard deviation in the radial fitting. The values of ε, δ, and R_m, for linear configuration, are 1.0493 kcal mol^{-1}, 29.856, and 12.527 au, respectively. The values of standard deviation in its ε, δ, and R_m are 0.02 kcal mol^{-1}, 1.3, and 0.0379 au, respectively, which are corresponding with 1.9%, 4%, and 0.3% error. The errors for the most stable configuration (cross) reaches to 0.24%, 0.03%, and 0.04% for ε, δ, and R_m, respectively. Figure 8 shows the comparison between the calculated extrapolated potential and the results obtained from the radial fitting for different configurations. It should be mentioned that the values of ε, δ, and R_m obtained from the fitting are different for each configuration. In the previous step, the values for the parameters (ε, δ, and R_m) were obtained as intermediate fitting parameters for different configurations. Now, each parameter of the potential (ε, δ, and R_m) is

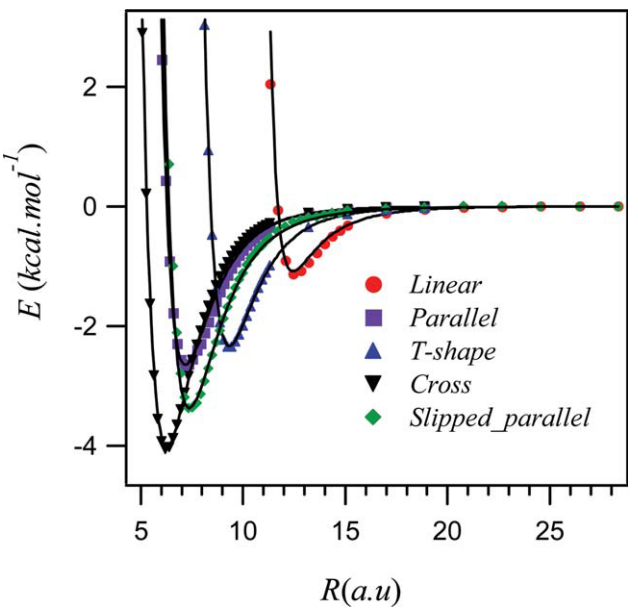

Figure 8. Radial dependence of the extrapolated intermolecular potential to the complete basis, calculated at the MP2 level of theory, for various configurations containing linear ($\alpha = \beta = \gamma = 0^\circ$), parallel ($\alpha = \beta = 90^\circ$ and $\gamma = 0^\circ$), T-shape ($\alpha = 0^\circ$, $\beta = 90^\circ$, and $\gamma = 0^\circ$), slipped parallel ($\alpha = 60^\circ$, $\beta = 120^\circ$, and $\gamma = 0^\circ$), and cross ($\alpha = \beta = 90^\circ$ and $\gamma = 90^\circ$) configurations. Solid lines correspond to the interaction potential function, obtained from the radial fitting. Symbols denote the extrapolated potential energy points.

classified based on the values of dihedral angle used in the *ab initio* calculations. Before starting the angular fitting of each parameter, the number of surface points of each parameter was increased by interpolating in α and β angles. The surface of each parameter, at a fixed value of dihedral angle, contains 49 points. More points are needed for a better display of the surface of each parameter; these can be obtained using the interpolation method. The number of surface points of each parameter at each dihedral angle increased to 1296 using the cubic spline interpolation method implemented in the Igor software. To check the validity of the interpolation method, we performed the *ab initio* calculations to obtain the intermolecular potential energy *versus* intermolecular distance for several intermediate geometries and then fitted them with Eq. (7) to obtain the values of ε, δ, and R_m. The obtained fitting parameters were compared with the values obtained from the interpolation, and a good agreement (a difference of less than 2–4%) between these values was found. Then, the interpolated surface of each parameter at each dihedral angle was fitted to the functional form of Eq. (8) via a damped Gauss–Newton-fitting procedure written in the Maple 9.5 software to obtain the values for the coefficients $Q_{l_a l_b l}$. In angular fitting, our aim was only to have a reasonable fitting in such a way that $Q_{l_a l_b l}$ coefficients along with Eq. (8) reproduce the potential parameters (ε, δ, and R_m) very well, but also to have an analytical expression to describe the topology of potential energy surface and use it easily to obtain the thermodynamic properties of CS_2 fluid. Because addition of higher order terms does not much improve the results, the angular series of Eq. (8) is truncated after the term with $l = 12$. 182 $Q_{l_a l_b l}$ coefficients were used in the second stage of the fitting program to obtain the desired accuracy. The accuracy of the resulting fit was checked by regenerating the potential parameters (ε, δ, and R_m) using the values of the coefficients $Q_{l_a l_b l}$ and comparing them directly with the values obtained from the first step. Over the entire grid, the differences are less than 1.4%, 0.43%, and 0.22% for ε, δ, and R_m, respectively, which is related to linear configuration. For example, the difference values for the parallel configuration are 0.04%, 0.23%, and 0.07% for ε, δ, and R_m respectively. Generally, the difference of the potential parameters is less than 0.5% for all configurations considered in this work (except ε parameter of linear configuration). Figure 9 shows α and β dependence of the parameters (ε, δ, and R_m) obtained from the first step of fitting, and compares them with the corresponding parameters obtained from the angular fitting. It is clear that the analytic function obtained here for ε, δ, and R_m can reproduce the values obtained from radial fitting very well.

$Q_{l_a l_b l}$ coefficients, obtained from the angular fitting, were used along with eqs. (7)–(9) to reproduce the 4D fitting potential energy surface for comparison with the calculated extrapolated MP2 potential energy surface. The value of root mean square deviation of 4D fitting is equal to 0.039 kcal mol^{-1} when 2790 points are considered on the potential energy surface. Also, the average absolute value of a difference between the calculated extrapolated MP2 energies and 4D fitting energies, taken over 2790 points, has been calculated to show the quality of fitting. The calculated value of average absolute value of a difference is about 0.025 kcal mol^{-1}, which shows that the fitted potential energy surface is accurate at the most stable configurations.

The characteristics of the minimum points on the 4D-fitted potential energy surface for configurations with the same dihedral angle (γ) have been listed in Table 1. It is found that the global minimum of the fitted potential energy surface is the ($\alpha = \beta = 90^\circ$, $\gamma = 90^\circ$, and $R = 6.23$ au) configuration with a well depth of 3.980 kcal mol^{-1}, which is different from the global minimum of the potential energy surface of CO_2 dimer ($\alpha = 59.8^\circ$, $\beta = 120.2^\circ$, $\gamma = 0^\circ$, and $R = 6.559$ au). The reason for this difference can be understood by analyzing the intermolecular potential in terms of its constituent components containing electrostatic, exchange-repulsion, induction, and dispersion to investigate their variations with the CS_2 dimer configuration in comparison with the CO_2 dimer, which will be the subject of a future study.

Some features of the potential energy surface can be observed in Figure 10 showing a three-dimension of the surface along with a two-dimensional cross-section for the value of the intermolecular separation $R = 9.33$ au and the dihedral angle $\gamma = 0$. As shown, the potential energy surface is symmetric with respect to the $\alpha = \beta$ surface. In the cross-section plot, the positions of linear (L), slipped parallel (P), parallel (H), and T-shape (T) configurations have been labeled on the figure. The characteristic points visible in Figure 10 have been listed in Table 2. Also, Figure 11 shows the cross-section with the same value of R but with the angle γ fixed at 90°.

Second Virial Coefficient

We have calculated the second virial coefficient $B_2(T)$ of CS_2 fluid over the range of experimentally measured temperatures using the extrapolated MP2 fitted potential energy surface to give a first, simple test of the quality of the calculated *ab initio* potential in this work. The classical contribution to $B_2(T)$ is calculated using the following expression[30]:

$$B_2(T) = -\frac{N_A}{4}\int_0^{\infty}\int_0^{\pi}\int_0^{\pi}\int_0^{2\pi} \times\left(\exp\left(-\frac{E(R,\alpha,\beta,\gamma)}{kT}\right)-1\right)R^2\sin\alpha\sin\beta dR d\alpha d\beta d\gamma \quad (10)$$

where, k and N_A are the Boltzmann and Avogadro constants. The quantum correction to $B_2(T)$ was expected to be small and hence ignored. Gaussian quadrature was used to integrate over the angles, whereas a Romberg method, based on the trapezoidal rule, was used to integrate over the radial coordinate. Integration over R was performed numerically between 3.8 and 57 au, with the region of $R < 3.8$ au approximated by the hard sphere expression. The number of angular and radial points was increased until the result was firmed.

The second virial coefficient $B_2(T)$ calculated via the fitted extrapolated MP2 potential energy surface has been reported in the fourth column of Table 3. It can be seen that the calculated second virial coefficient has a considerable negative deviation from the experimental results (the second and third columns of Table 3). This means that there is an additional attraction in the extrapolated MP2 potential because of the exaggeration of the

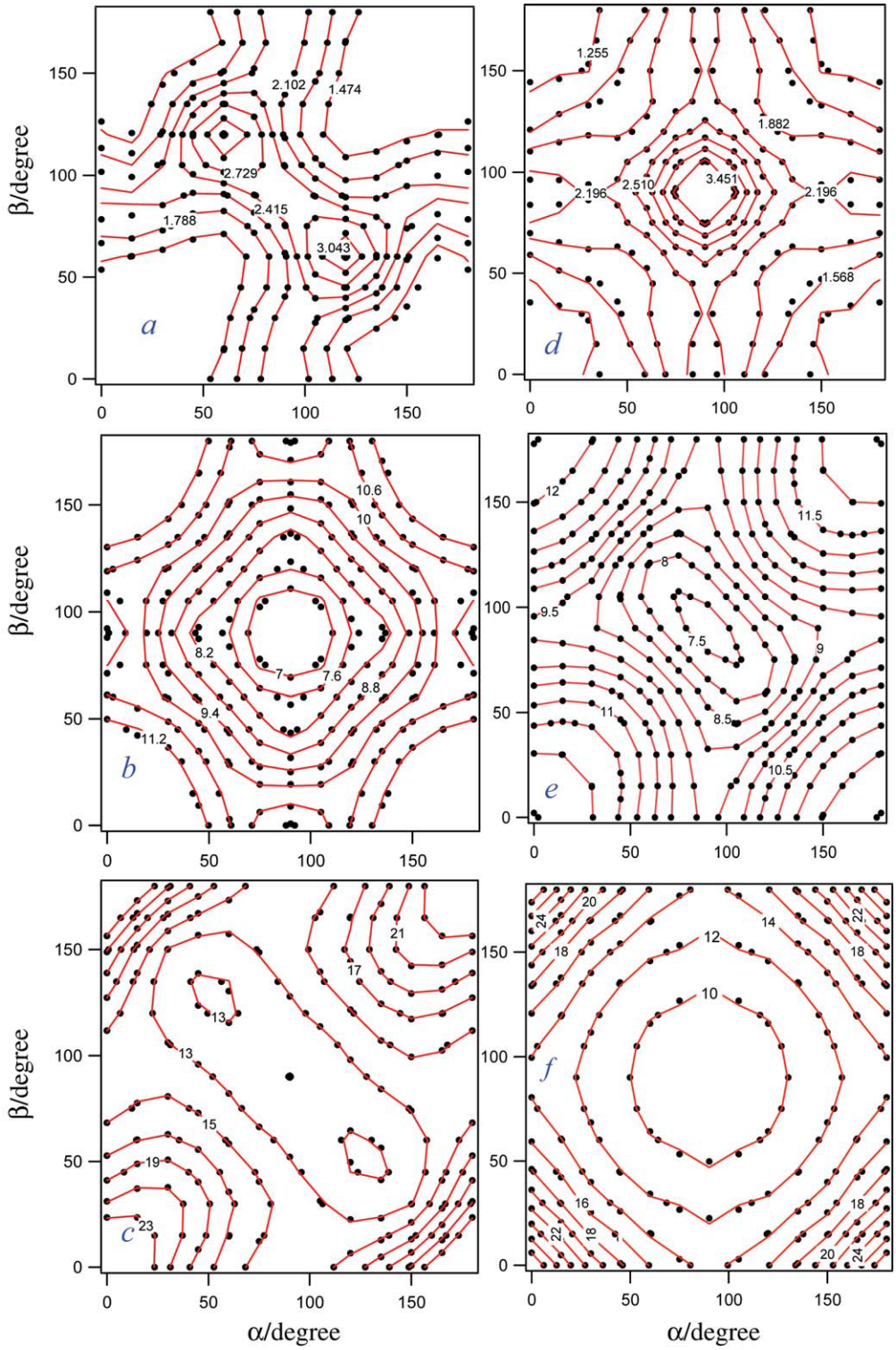

Figure 9. Contour plots of ε, δ, and R_m. (*a*) ε, (b) R_m, and (c) δ for configurations with the dihedral angle $\gamma = 0^\circ$; and (*d*) ε, (e) R_m, and (f) δ for $\gamma = 90^\circ$. Symbols are parameters obtained from the radial fitting, and lines show the angular fitting results. [Color figure can be viewed in the online issue, which is available at wileyonlinelibrary.com.]

Table 1. Positions of the Minimums on the Fitted Extrapolated MP2 Potential Energy Surface for Each Value of γ Along With Their Associated Interaction Energies.

R (au)	α (°)	β (°)	γ (°)	E (kcal mol^{-1})
7.85	61.8	118.9	0	3.363
7.35	64.11	115.95	30	3.066
6.42	90.00	90.00	60	3.833
6.23	90.00	90.00	90	3.980

Table 2. The Position of the Points Labeled on Figure 10 and Their Associated Interaction Energies.

Label point	R (au)	α (°)	β (°)	γ (°)	E (kcal mol^{-1})
L	9.33	0	0	0	724.681
T	9.33	0	90	0	−2.157
H	9.33	90	90	0	−1.129
P	9.33	128.79	52.105	0	−2.669

correlation energy. After scaling the extrapolated MP2 potential energy surface according to Eq. (6), using the global scaling factor (0.578) to obtain the extrapolated potential energy surface at the QCISD(T) level of theory, the calculated $B_2(T)$ (the fifth column of Table 3) is in good agreement with the experimental results reported by Dymond and Smith.[2] However, there is a minor deviation from the measured values of Hajjar et al.[3] over the entire temperature range, from 313.15 to 473.15 K for which we suggest that the experimental values of Hajjar et al.[3] should be re-examined. At the lowest temperature, the uncertainty of measurements reported in ref. 2 is only 30 cm^3 mol^{-1}, and these values are in better agreement with our theoretical values.

Again, the good agreement between the experimental and calculated second virial coefficients confirms that the shape of the potential energy surface for CS_2 dimer is approximately independent of the theoretical levels used in this work, and we can approximate the QCISD(T) level by scaling the MP2 potential energy surface.

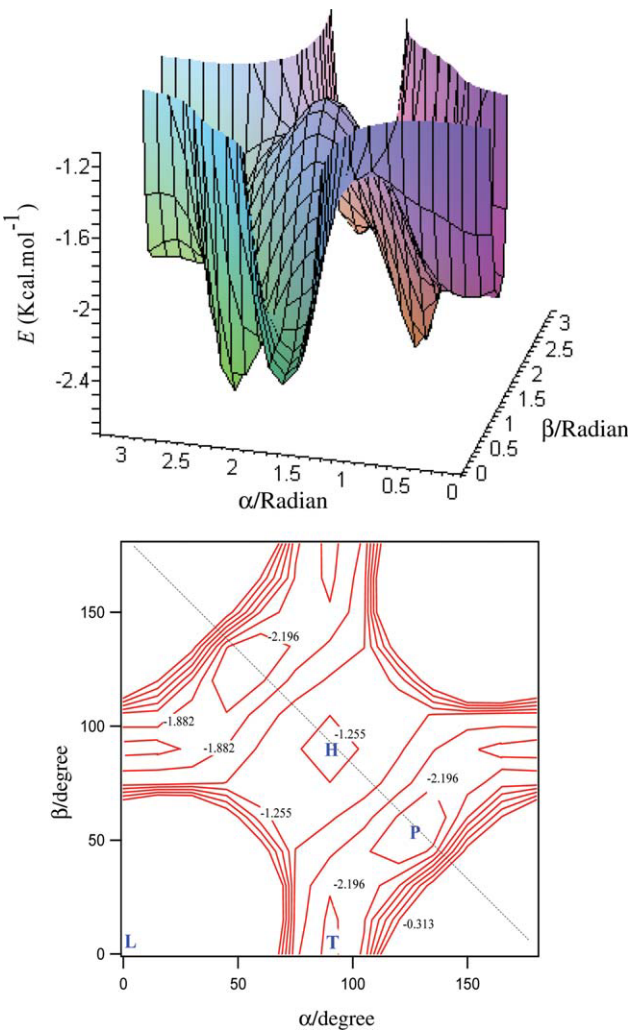

Figure 10. A three dimentional plot of fitted potential energy surface along with its contour plot. The position of selected configurations have been shown on the contour plot. The distance R fixed at 9.33 au and the angle γ fixed at 0. The contours are symmetric with respect to the dashed line. The energy labels are in atomic unit. [Color figure can be viewed in the online issue, which is available at wiley onlinelibrary.com.]

Isotropic Dipole–Dipole Dispersion Coefficient

The value of isotropic dipole–dipole dispersion coefficient C_6 ($l_a = 0, l_b = 0, l = 0$) has been obtained from the calculated *ab*

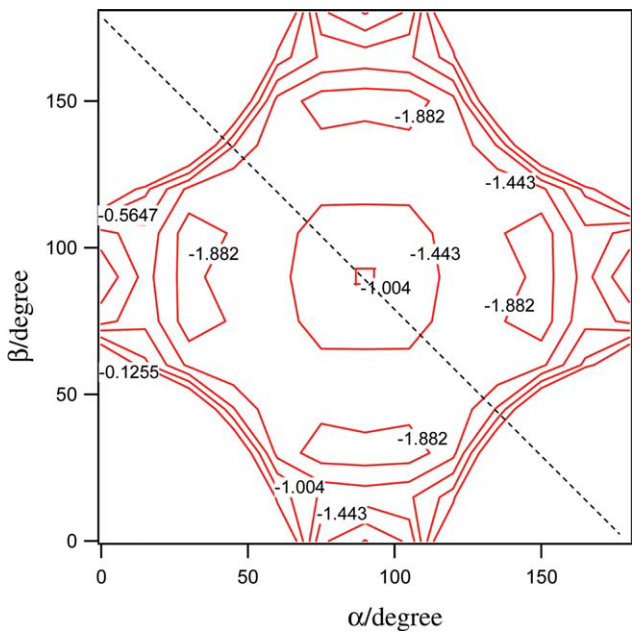

Figure 11. Same as Figure 10 with the angle $\gamma = 90°$. [Color figure can be viewed in the online issue, which is available at wileyonlinelibrary.com.]

Table 3. Temperature Dependence of the Second Virial Coefficient $B(T)$ ($cm^3\ mol^{-1}$) (Experimental and Calculated Values).

T (K)	B_2[a]	B_2[b]	This work[c]	This work[d]	This work[e]	This work[f]
280	−930	–	−3637.52	−909.082	−934.792	−923.277
290	−862	–	−3366.62	−847.18	−848.777	−847.445
300	−796	–	−3042.82	−792.16	−775.488	−781.953
310	−740	–	−2766.56	−743.068	−712.481	−724.937
313.15	–	−810	−2704.53	−730.328	−697.991	−711.25
323.15	–	−700	−2479.4	−686.798	−643.748	−661.72
325	−666	–	−2425.26	−678.567	−633.235	−652.196
337.15	–	−605	−2205.67	−632.396	−578.146	−601.182
350	−567	–	−1994.06	−590.198	−531.132	−556.583
353.15	–	−480	−1945.76	−578.62	−516.245	−543.181
368.15	–	−430	−1746.48	−535.311	−469.027	−498.121
375	−489	–	−1680.08	−519.677	454.953	−483.652
382.15	–	−380	−1593.25	−500.191	−432.786	−462.874
398.15	–	−335	−1449.76	−465.261	−398.713	−429.075
400	−429	–	−1442.52	−462.122	396.300	−426.439
413.15	–	−310	−1339.02	−436.526	−372.038	−402.15
427.15	–	270	−1250.42	−412.309	−350.125	−379.852
430	−377	–	−1226.06	−405.721	341.841	−372.391
453.15	–	−230	−1104.89	−371.186	−312.021	−341.546
473.15	–	−195	−991.646	−340.239	−280.123	−310.822

[a]Reference 2.
[b]Reference 3.
[c]Extrapolated MP2 potential energy surface.
[d]Scaled extrapolated MP2 potential energy surface.
[e]Global Lennard-Jones potential.
[f]Global exp-6 potential.

initio extrapolated MP2 potential energy surface. To do this, we used the method applied by Hellman et al.[31] By considering that the contribution of electrostatic interaction, overlap (exchange repulsion and electrostatic interactions deviating from the classical multiple expansion), quadrupole–dipole dispersion (C_8), and quadrupole–quadrupole dispersion (C_{10}) are negligible at enough long range intermolecular separation, the variation of $E(R)$ *versus* ($1/R^6$) will be linear for each dimer configuration, and the slope of the line is approximately equal to the true C_6 value of that configuration. The extrapolated MP2 values of $E(R)$ were plotted *versus* ($1/R^6$) for each dimer configuration separately to obtain its C_6 value. The C_6 values of different dimer configurations were fitted using eqs. (8) and (9). The angular series of Eq. (8) was truncated after the term with $l = 12$. 182 $Q_{l_a l_b l}$ coefficients were used in the angular fitting to obtain the desired accuracy. The obtained isotropic value of C_6 ($l_a = 0, l_b = 0, l = 0$) is about 1610.56 au, which is comparable with the value obtained at the MP2 level of theory (1533 au) using Casimir–Polder integral.[32] The calculated value of C_6 ($l_a = 0, l_b = 0, l = 0$) using continuous dipole oscillator strength distribution (DOSDS) is about 871 au.[33] To the best of our knowledge, there is no experimental value for isotropic C_6 coefficient of CS_2 in the literature, but it has been determined that the values that are obtained using DOSDS are accurate 1–2% by comparison between different sets of experimental data.[33]

It is seen that there is about 84% error in the isotropic C_6 value obtained using extrapolated MP2 potential energy surface in comparison with the value obtained using DOSDS method. This value of error is reasonable because one of the serious shortcomings of MP2 theory is a noticeable overestimation of dispersion energy. The scaled MP2 isotropic C_6 value, obtained using the global scaling factor (0.578), is about 930.903 au, which has about 8% error in comparison with the value reported in reference.[33] This comparison also confirms that the selected global scaling factor is approximately correct, and increasing the quality of the computational level does result in a simple scaling of the potential energy surface in the CS_2-CS_2 system.

Spherical One-Center Representation of Potential Energy Surface

As explained before, the potential energy surface of dimer *versus* its configuration (α, β, γ, and R) can be calculated using eqs. 7–9. This analytical form, however, is too complicated because the angular function of each parameter in the exp-6 potential has 182 parameters. Therefore, it is useful to have a simple analytical spherical one-center intermolecular potential, which can represent the interaction accurately and allow the potential functional to be easily implemented in thermodynamic relations for the calculation of equilibrium and nonequilibrium properties of fluids. Furthermore, it is simply used in the molecular dynamics and Monte Carlo simulations. To the best of our knowledge, there is no spherical one-center intermolecular potential for CS_2 fluid in the literature.

To do this, we used the global fitting method similar to Shadman et al.'s work,[34] but using weighting factor for each energy point. The fitting was performed using the global fitting program implemented in the Igor 6.01 software. Global fitting is an operation whereby multiple data sets are simultaneously fit, typically to a fitting function model while sharing all of the fitting parameters between data sets. In fact, multiple data sets are fitted with one model simultaneously. For this purpose, we considered the exp-6 potential as the model, and the parameters of the potential were obtained by radial fitting of the intermolecular interaction potential of all configurations with exp-6 potential simultaneously. We used the following Boltzmann weighting factor to favor the regions of the potential well to the high repulsive regions.

$$W_{ij}(E) = e^{-\frac{E_{ij}^{\mathrm{cal}}}{E_{\mathrm{b}}}} \tag{11}$$

The potential parameters as well as E_{b} change in such a way that to minimize the following function for all the configurations simultaneously:

$$\chi = \frac{\sum_{i=1}^{N1}\sum_{j=1}^{N2} W_{ij}\left(E_{ij}^{\mathrm{cal}} - E_{ij}^{\mathrm{ab}}\right)}{\sum_{i=1}^{N1}\sum_{j=1}^{N2} W_{ij}} \tag{12}$$

where, E_{cal} is the interaction energy obtained from Eq. (7) and E_{ab} is the *ab initio* interaction energy. N_1 is the total number of dimer configurations and N_2 is the number of intermolecular dis-

Table 4. The List of Potential Parameters for the Potential Models Lennard-Jones (LJ) and Exp-6 Obtained in this Work.

Potential forms	Potential parameters		E_b (kcal mol^{-1})
Exp-6	ε (kcal mol^{-1})	1.621 ± 0.062	4.0788
	R_m (au)	6.555 ± 0.0321	
	α	9.300 ± 0.32	4.0788
LJ	ε (kcal mol^{-1})	1.902 ± 0.08	
	σ (au)	5.459 ± 0.015	

tances. During the fitting, the second virial coefficient is calculated at different temperatures and compared with the experimental results of Dymond and Smith.[2] The same procedure was used to obtain the parameters of the LJ potential, which has the following functional form:

$$E_{lj}(R) = 4\varepsilon\left[\left(\frac{\sigma}{R}\right)^{12} - \left(\frac{\sigma}{R}\right)^{6}\right] \quad (13)$$

The potential parameters obtained from the global fitting of the exp-6 and LJ potentials as well as their E_b are reported in Table 4. As seen in Table 4, the position of the minimum energy of LJ and exp-6 potentials is nearly about the minimum energy position of cross configuration (the most stable configuration), and the value of E_b is the same for them. This means that the cross configuration has the most weight in the global fitting in comparison with the other configurations.

The second virial coefficients calculated using parameterized exp-6 and LJ potentials obtained from the global fitting are compared with the experimental data in Table 3. The experimental data of $B_2(T)$ available are lower than the Boyle temperature. As shown in Table 3, the second virial coefficients calculated via the global exp-6 and LJ potentials are more consistent with the experimental results of ref. 2, but the exp-6 values of $B_2(T)$ are in better agreement with those of ref. 2 than with the values calculated via the LJ potential.

Conclusions

A new intermolecular potential energy surface for the CS_2 dimer has been calculated using the supermolecular approach under consideration of the BSSE. MP2 level of theory has been used with two different basis sets of the correlation-consistent series of Duning (aug-cc-pVDZ and aug-cc-pVTZ) to calculate the energy points. We used the results for the two different basis sets to extrapolate the potential energy surface to the CBS limit. The effect of more computationally intensive quantum chemical methods such as QCISD(T) and CCSD(T) levels of theory on the potential energy surface were investigated. It was found that the MP2 level of theory overestimates the potential energy surface by a factor of nearly 1.73 in comparison with the QCISD(T) and CCSD(T) methods. The reason for this behavior is the exaggeration of correlation energy, which exists in the MP2 level of theory. However, it was shown that the shape of the potential energy surface was approximately well reproduced at the lower level of theory and that the QCISD(T) intermolecular potential energy surface was well approximated by scaling the MP2 potential energy surface and, therefore, accurate quantitative results could be obtained.

The extrapolated interaction energies for different configurations and radial distances were used in a fitting procedure to obtain the angular dependency of the parameters of the exp-6 potential. In addition, a simple spherical potential model for the system considered in this work was obtained by global fitting of the radial dependence of extrapolated interaction energies for different configurations to the LJ and exp-6 potentials. Values of the second virial coefficient, as calculated by the scaled MP2 potential surface and the global potentials, provide a good description of the available experimental data. Finally, the value of isotropic dipole–dipole dispersion coefficient was obtained from the extrapolated MP2 potential energy surface and compared with the corresponding value obtained using continuous DOSDS. This comparison shows that the MP2 theory overestimates the dispersion energy.

Acknowledgments

The authors would like to thank the Isfahan University of Technology. Also, they acknowledge generous allocations of computing from the Australian National Computational Infrastructure. HF would like to thank Prof. M. Tabrizchi for valuable discussions.

References

1. Hedrick, J. L.; Mulcahey, L. J.; Taylor, L. T. Mikrochim Acta 1992, 108, 115.
2. Dymond, J. H.; Smith, E. B. The Virial Coefficients of Pure Gases and Mixtures; Clarendon Press: Oxford, 1980.
3. Hajjar, R. F.; Kay, W. B.; Leverett, G. F. J Chem Eng Data 1969, 14, 377.
4. Zhu, S.-B.; Lee, J.; Robinson, G. W. Mol Phys 1988, 65, 65.
5. Hoinkis, J.; Ahlrichs, R.; Böhm, H.-J. Int J Quantum Chem 1983, 23, 821.
6. Peebles, S.; Peebles, R. J Mol Struct 2007, 830, 176.
7. Bock, S.; Bich, E.; Vogel, E. Chem Phys 2000, 257, 147.
8. Hashimoto, M.; Isobe, T. Bull Chem Soc Jpn 1974, 47, 40.
9. Brigot, N.; Odiot, S.; Walmsley, S. H.; Whitten, J. L. Chem Phys Lett 1977, 49, 157.
10. Illies, A. J.; McKee, M. L.; Schlegel, H. B. J Phys Chem 1987, 91, 3489.
11. Hiraoka, K.; Shoda, T.; Morise, K.; Yamabe, S.; Kawai, E.; Hirao, K. J Chem Phys 1986, 84, 2091.
12. Oakley, M. T.; Wheatley, R. J. J Chem Phys 2009, 130, 034110.
13. Moller, C.; Plesset, M. S. Phys Rev 1934, 46, 618.
14. Dunning, T. H.; Peterson, K. A.; Wilson, A. K. J Chem Phys 2001, 114, 9244.
15. Frisch, M. J.; Trucks, G.W.; Schlegel, H.B.; Scuseria, G.E.; Robb, M.A.; Cheeseman, J.R.; Montgomery, J.A.; Vreven, Jr., T.; Kudin, K.N.; Burant, J.C.; Millam, J.M.; Iyengar, S.S.; Tomasi, J.; Barone, V.; Mennucci, B.; Cossi, M.; Scalmani, G.; Rega, N.; Petersson, G.A.; Nakatsuji, H.; Hada, M.; Ehara, M.; Oyota, K.; Fukuda, R.; Hasegawa, J.; Ishida, M.; Nakajima, T.; Honda, Y.; Kitao, O.; Nakai, H.; Klene, M.; Li, X.; Knox, J.E.; Hratchian, H.P.; Cross, J.B.; Bakken, V.; Adamo, C.; Jaramillo, J.; Gomperts, R.; Stratmann,

R.E.; Yazyev, O.; Austin, A.J.; Cammi, R.; Pomelli, C.; Ochterski, J.W.; Ayala, P.Y.; Morokuma, K.; Voth, G.A.; Salvador, P.; Dannenberg, J.J.; Zakrzewski, V.G.; Dapprich, S.; Daniels, A.D.; Strain, M.C.; Farkas, O.; Malick, D.K.; Rabuck, A.D.; Raghavachari, K.; Foresman, J.B.; Ortiz, J.V.; Cui, Q.; Baboul, A.G.; Clifford, S.; Cioslowski, J.; Stefanov, B.B.; Liu, G.; Liashenko, A.; Piskorz, P.; Komaromi, I.; Martin, R.L.; Fox, D.J.; Keith, T.; Al-Laham, M.A.; Peng, C.Y.; Nanayakkara, A.; Challacombe, M.; Gill, P.M.W.; Johnson, B.; Chen, W.; Wong, M.W.; Gonzalez, C.; Pople, J.A. Gaussian 03, Revision B03; Gaussian Inc.: Pittsburgh, PA, 2004.
16. Lide, D. R. CRC Handbook of Chemistry and Physics, 88th ed.; CRC Press: Boca Raton, FL, 2008.
17. Tsuzuki, S.; Uchimaru, T.; Mikami, K.; Tanabe, K. J Chem Phys 1998, 109, 2169.
18. Tsuzuki, S.; Uchimaru, T.; Mikami, K.; Tanabe, K. J Chem Phys 1999, 110, 11906.
19. Boys, S. F.; Bernardi, F. Mol Phys 1970, 19, 553.
20. Jensen, F. Theor Chem Acta 2005, 113, 267.
21. Helgaker, T.; Jorgensen, P.; Olsen, J. Molecular Electronic Structure Theory; John Wiley & Sons: New York, 2000.
22. Tao, F. Int Rev Phys Chem 2001, 20, 617.
23. Koch, H.; Fernandez, B.; Christiansen, O. J Chem Phys 1998, 108, 2784.
24. Tsuzuki, S.; Uchimaru, T.; Mikami, M.; Tanabe, K. J Phys Chem A 2002, 106, 3867.
25. Tulegenov, A. S.; Wheatley, R. J.; Hodges, M. P.; Harvey, A. H. J Chem Phys 2007, 126, 094305.
26. Cremer, D.; He, Z. J Phys Chem 1996, 100, 6173.
27. Domaski, K. B.; Kitao, O.; Nakanishi, K. Mol Sim 1994, 12, 343.
28. Stone, A. J. The Theory of Intermolecular Force; Oxford University Press: Oxford, 2002.
29. Buckingham, A. D.; Fowler, P. W.; Hutson, J. M. Chem Rev 1988, 88, 963.
30. Ben-Naim, A. Statistical Thermodynamics for Chemist and Biochemists; Plenum Press: New York, 1992.
31. Hellmann, R.; Bich, E.; Vogel, E. J Chem Phys 2008, 128, 214303.
32. Tkatchenko, A.; DiStasio, R. A., Jr.; Head-Gordon, M.; Scheffler, M. J Chem Phys 2009, 131, 094106.
33. Kumar, A.; Meath, W. J. Chem Phys 1984, 91, 411.
34. Shadman, M.; Yeganegi, S.; Ziaie, F. Chem Phys Lett 2009, 467, 237.
35. Maitland, G. C.; Rigby, M.; Smith, E. B.; Wakeham, W. A. Intermolecular Forces; Claren Press: Oxford, 1987.